J. Min. Metall. Sect. B-Metall., 56 (1) (2020) 89 - 97

Journal of Mining and Metallurgy, Section B: Metallurgy

EFFECT OF COLD ROLLING AND ANNEALING TEMPERATURE TO THE CHARACTERISTICS OF α + β′ PHASES IN Cu-29.5Zn-2.5Al ALLOY PRODUCED BY GRAVITY CASTING

I. Angela [a], I. Basori [b], B. T. Sofyan [a,*]

[a] Universitas Indonesia, Department of Metallurgy and Materials Engineering, Faculty of Engineering, Depok, Indonesia

[b] Universitas Negeri Jakarta, Department of Mechanical Engineering, Faculty of Engineering, Jakarta, Indonesia

(Received 20 August 2018; accepted 09 July 2019)

Abstract

Al-brass alloys (Cu29.5Zn2.5Al wt. %) were produced by gravity casting and homogenized at 800 °C for 2 h, resulting in a binary phase morphology identified as cubic α and martensitic β′ phases through X-ray diffraction (XRD). Samples were then subsequently cold rolled and annealed at 150, 300, 400, and 600 °C for 30 minutes. Visible traces of slip, intersecting slip bands, and shear bands were observed in microstructure images of the samples after each progressive deformation stage. Deformation-induced martensites were present after 20 % cold rolling. Higher thickness reduction resulted in simultaneous strain hardening of the phases. Low temperature annealing slightly increased microhardness, of both α and β′, due to the formation of precipitates. SEM-EDX analysis showed that no solute segregation was found in annealed samples. Annealing at higher temperature resulted in conventional softening. Recrystallized equiaxed β′ phase grains were visible after annealing at 600 °C.

Keywords*: Aluminium; Brass; Homogenization; Martensitic; Cold rolling; Annealing*

1. Introduction

Possessing exceptional mechanical properties, cartridge brass (Cu28Zn wt. %) alloys are used widely in high-service applications e.g. low pressure valves, heat exchanger pipes, and condensers which involve extensive deformation during their manufacture. Previous studies were conducted to improve the formability of cartridge brass through alloying using Mn [1], Bi [2], and Al [3], with the optimum combination of strength and ductility properties found in duplex brass with 1.9 wt. % Al [3]. However, the aforementioned research did not discuss the crystallographic structure of each phase mentioned in this study: microhardness measurements and X-ray diffraction (XRD) analysis. Many studies showed brass with high alloying contents (up to 35 wt. % Zn) contains fcc α and relatively strong ordered β′ phase at room temperature [4-5].

Brass has an interesting deformation mechanism that differs with each progressing thickness reduction level. Mo et al. [6] observed the presence of three stages of deformation mechanism on the cold rolling of Cu28Zn2.1Al wt. % alloys. Slip, deformation twins, and shear bands appeared after 25 %, 35 %, and 50 % reduction, respectively. The presence of Zn and Al significantly lowered the high stacking fault energy (γ-SFE) of the Cu matrix, hence a shift from slip to twinning was observed [7]. Further increase in deformation eventually caused shear banding since the extensive twinning inhibited the formation of slip [8-9].

In order to diminish the risk of cracking and stress-induced corrosion, thermal annealing is traditionally used to recover high residual stress density after cold deformation [10-11]. A good control of annealing temperature and its duration is strictly required to achieve the desired mechanical properties, especially for annealing of duplex brass which has phases with varying SFE values [7]. The presence of thermal energy during annealing enables dislocation to disentangle, so that alloys are softened. An appreciable increase of ductility was found after annealing of 70 % cold-rolled Cu28Zn wt. % at 150-500 °C for 30 min [8] and short-annealing of cryorolled Cu18Zn wt. % at 225-300 °C for 20 min. [12]. Unusually, the anneal hardening effect was encountered by Gong et al. [13] in his investigation on short-temperature annealing of heavily cryo-rolled CuZn*x*Al alloys. This peculiar hardening was attributed to a dense population of annealing twins and stacking faults along with the

*Corresponding author: bondan@eng.ui.ac.id

https://doi.org/10.2298/JMMB180820037A

formation of solute segregation during annealing of 94 % cryorolled Cu23.89Zn1.86Al wt. % at 150-200 °C for 1 h.

Based on the above literature survey, this research performed phase characterization and analysis on deformation mechanism and annealing behavior of duplex Al-brass alloys.

2. Experimental procedure

Cu29.5Zn2.5Al wt. % alloys were produced by gravity casting using commercially available 99.9 % Cu rods, high purity Zn, and Al ingots supplied by Korea Zinc Co., Ltd., and Inalum Co., Ltd., adhered with borax flux to protect the melt from oxidation. Starting materials were melted in induction furnace at 1150 °C and cast in an 800 °C preheated AISI H 13 steel mold. As-cast plates of 6 mm thickness were then homogenized at 800 °C for 2 h and air cooled to eliminate segregation to attain uniform alloy microstructures. Optical emission spectroscopy (OES) composition analysis was done to the homogenized samples and the results are shown in Table 1. Samples were then subjected to cold rolling for 20 %, 40 %, and 50 % thickness reduction, followed by annealing at 150, 300, 400, and 600 °C for 30 min for specimen with 50 % deformation. Specimens were prepared using standard metallographic preparation with Al_2O_3 suspension for polishing and a ferric chloride (5 g $FeCl_3$ + 10 mL HCl 1 MM + 100 mL H_2O) etchant. Characterization was done using a Carl-Zeiss Primotech optical microscope, FEI Inspect F50 field emission scanning electron microscope (FE-SEM) and AMETEX-EDAX TSL energy dispersive x-ray spectroscopy (EDX) instrument in the Center of Metal Processing and Failure Analysis (CMPFA) of Universitas Indonesia, CuKα XRD analysis for phase identification in PUSPIPTEK BATAN Indonesia, and Vickers microhardness measurement.

3. Results and discussion

3.1 Phase identification

Data from Table 1 were used to calculate with Scheil equation and plotted on the ternary Al-Cu-Zn equilibrium diagram by Liang and Schmid-Fetzer [14] to predict the phases after solidification, which indicated that the Cu29.5Zn2.5Al wt. % alloys consisted of binary α + β phases. Fig. 1 shows microstructures of both as-cast and as-homogenized Cu29.5Zn2.5Al wt. % alloys, showing the duplex structure. The light-colored phase in Fig. 1 (b) had a distinct lath martensitic shape in a basket weave-like pattern [15]. Ahlers [16] found that the martensitic transformation occurred in the disordered bcc β. During cooling, the high temperature bcc β went through order-disorder transitions into superlattices A2 → B2 → DO_3 (β_1) or $L2_1$ (β_3), depending on the initial alloy composition and cooling rate, that furthermore transformed into martensitic structure on reaching the martensite start (M_s) temperature [16-19]. Yakovsteva et al. [20] determined the transformation start temperature of the bcc β → β′ reaction as 454 °C based on isothermal sections for 550 °C and 600 °C of the Cu-Zn-Al ternary phase diagram calculated using Thermo-Calc. This high M_s temperature was possible due to the existence of Al inclusions in the alloys, as reported by Haberkorn et al. [21]. Additionally, this martensitic transformation could result in different martensite variants, depending on the initial alloy composition [22]. Martensite stacks M9R and M18R are the most common to form in brass and Al-brass alloys due to their high stability [16]. Thus, the light-colored phase was assumed to be M9R/M18R which resulted from β phase transformation (and is called β′ in this paper) hence the dark-colored area was inferred as the α phase. Fig. 1 shows that the β′ phase in as-homogenized samples was smaller and more needle-like than in the as-cast samples. Quantitative analysis done on as-cast and as-homogenized images using *Image Pro Analysis* software indicated an equal α:β′ phase volume ratio of 35:65 in both samples, showing that homogenization did not induce change in phase volume fraction. This agreed with Wayman and Duerig [18] who explained that volume fraction of transformed phase in martensitic transformation, which was a form of displacive solid-state transformation, would only be dependent on the composition of the initial alloy as well as temperature, and it was not influenced by the length of holding time in the given temperature.

Fig. 2 and Table 2 show the results of XRD analysis on the as-cast and as-homogenized Al-brass samples, confirming the presence of M9R and M18R martensites, as well as cubic α phase in both specimens [23]. No existence of cubic β was found. Data labels in Fig. 2 represent the phase identity and Miller indices (numbers in brackets) of each peak obtained from data analysis using X'Pert HighScore Plus v2.2.3 software and a research by Natali et al. [24]. Predominant peaks were identified as M18R, although further quantitative line profile analysis (LPA) is needed to determine the exact volume fraction of each phase. No cubic β peaks were found in the XRD results. This finding also agreed with Haberkorn et al. [21] stating that Al inclusion in Cu30Zn alloys expanded the equilibrium region of the β parent phase, allowing a large range of M_s temperature of -273 to 423 °C, hence the use of slow cooling (in this work: air cooling) was appropriate for the martensite to form.

Table 1. *Nominal composition of the Cu29.5Zn2.5Al (wt. %) alloys*

Composition (wt. %)									
Zn	Al	Pb	Sn	Fe	Bi	Ag	Co	Zr	Cu
29.50 ± 0.03	2.51 ± 0.03	< 0.01	0.01	0.01	0.09	0.01	0.01	< 0.01	67.80 ± 0.06

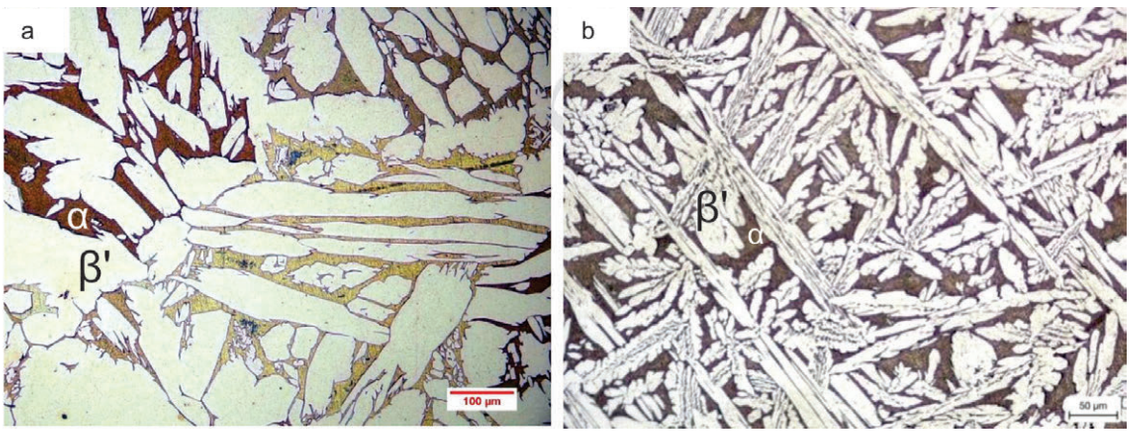

Figure 1. *Microstructures of (a) as-cast and (b) as-homogenized Cu29.5Zn2.5Al alloys showing the duplex morphology consisting of α + β′ phases*

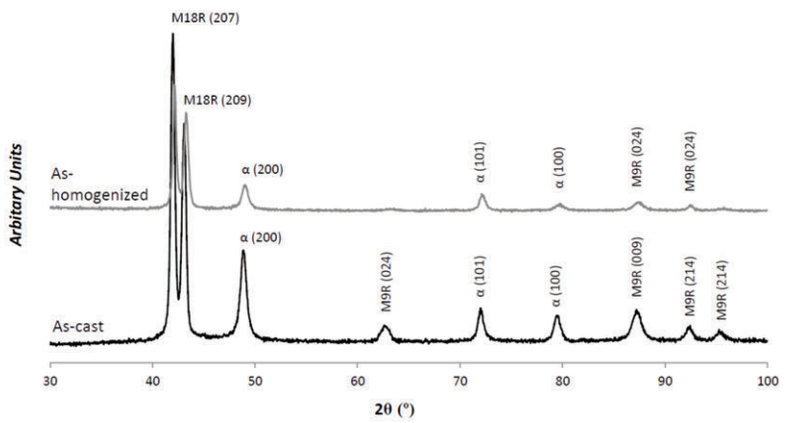

Figure 2. *XRD results of as-cast and as-homogenized Cu29.5Zn2.5Al wt. % alloys with peaks showing the existence of α + β′ (M9R and M18R)*

Table 2. *Lattice parameters of phases in as-cast and as-homogenized Cu29.5Zn2.5Al wt. % alloys*

AS-CAST					AS-HOMOGENIZED				
2θ (°)	*a* (Å)	*c* (Å)	*β* (°)	Phase	2θ (°)	*a* (Å)	*c* (Å)	*β* (°)	Phase
41.98	4.536	38.388	90	M18R	42.14	4.58	39.011	90	M18R
43.12	4.435	38.389	90	M18R	43.28	4.921	38.911	90	M18R
48.86	3.722	3.722	90	α	49.17	9.339	9.339	90	α
62.72	4.536	17.969	90	M9R	-	-	-	-	-
72.07	3.722	3.722	90	α	72.14	9.339	9.339	90	α
79.55	9.123	9.123	90	α	79.7	9.582	9.582	90	α
87.31	4.385	21.603	90	M9R	87.35	4.379	20.786	90	M9R
92.35	4.553	19.518	90	M9R	92.35	4.921	21.758	90	M9R
95.38	4.553	19.518	90	M9R	-	-	-	-	-

Table 3. *Microhardness of α and β′ phases in as-cast and as-homogenized Cu29.5Zn2.5Al wt. % alloys*

Remarks	Microhardness (HV)	
	α	β′
As-cast	103 ± 1	185 ± 1
As-homogenized	117 ± 1	190 ± 2

Vickers microhardness measurements on phases of both as-cast and as-homogenized specimens are shown in Table 3. The α (dark-colored region) had lower hardness than the major light-colored β′ phase. Smirnov et al. [5] found that microhardness of α and β′ phases of Cu12.68Zn5.27Al7.04Mn wt. % alloys produced by hot extrusion and annealed at 480 °C for 3 h ranged from 130-146 and 200-275 HV, respectively, agreeing with the trend of this work.

3.2 Deformation mechanisms

Fig. 3 shows the microstructures of cold rolled Cu29.5Zn2.5Al wt. % specimens at various thickness reduction levels. Evidence of slip, intersecting slip bands, and shear bands (SB) were identified to appear progressively in the OM images with increased deformation. At 20 % reduction, planar slip bands were observed in the α-phase region (on areas marked with dashed black rectangular in Fig. 3 (a)). Due to the low stacking fault energy (SFE) in Cu30Zn (SFE_{Cu} = 78 mJ/mm^2; $SFE_{Cu\text{-}30Zn}$ = 14 mJ/m^2 [25]), partial dislocations were widely separated from each other, hindering the formation of cross-slip and caused dislocations to organize themselves into planar slip bands [26] as observed in this work. Furthermore, fcc α had 12 slip systems and a close-packed atomic structure which facilitated slip [27] while β′ had a monoclinic structure with only three main slip systems, making it very difficult for slip in β′ [28]. In addition, needle-like martensite was also visible after 20 % deformation (Fig. 3 (b)). The applied stress during deformation possibly induced martensitic transformation in α.

As seen in Fig. 3 (c-f), further thickness reduction of 40 and 50 % also resulted in deformation traces in the soft α-phase. Evidence of intersecting slip bands were found after 40 % deformation. According to Suwas and Ray [29], with the progress of deformation, slip might occur simultaneously on more than one slip system, resulting in intersecting slip bands as marked with dashed circle in

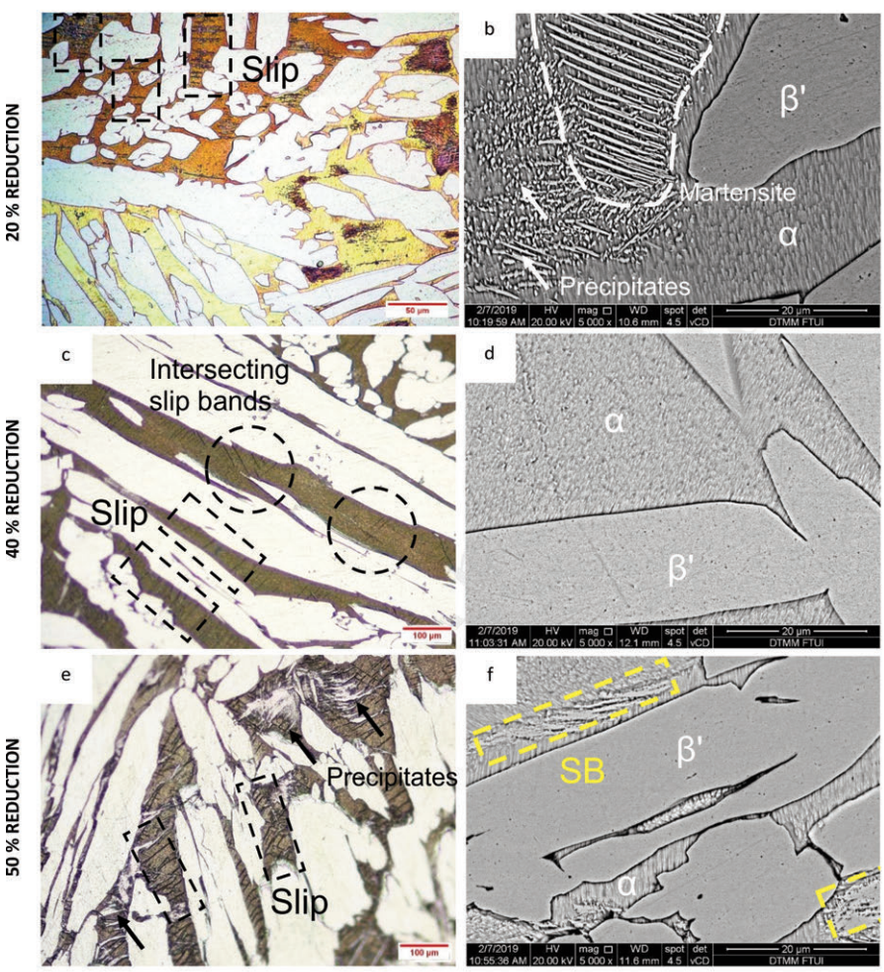

Figure 3. *Optical and Critical Dimension/CD-SEM images of Cu29.5Zn2.5Al wt. % alloys subjected to cold rolling with (a-b) 20 %; (c-d) 40 %; and (e-f) 50 % thickness reduction showing traces of slip, intersecting slip bands, shear bands (SB), precipitation, and deformation-induced martensite in the α phase (in area marked with white dashed line)*

Fig. 3 (c). In homogenous band-like shapes appeared at highest reduction level (Fig. 3 (f)), marked with yellow dashed rectangles. They were solely found inside the α-grains, and were identified as shear bands (SB), which occurred due to the heavy deformation. In cold rolled Cu-40Zn wt. %, Engler and Jensen [30] found that deformation texture would be intensified on the α-phase due to the existence of the hard β-phase. It is presumed that the subjected deformation load was localized in α-phase region due to the difference of strength and plasticity between the two phases, explaining why deformation was only visible in α [5]. Deformation was also responsible for the formation of precipitates (fine light shapes) on deformed areas as seen in Fig. 3 (b, e). Identities of the precipitates were possibly: fct α′, γ_2, or γ'_3 phase as described by Ahlers [16]. However, further phase examination using TEM has to be done in future study to confirm the identity of the precipitates.

A slight shift of α:β′ ratio was found on the rolled specimens. The α:β′ volume fraction ratios for as-homogenized and deformed samples were 35:65 and ~30:70, respectively. According to Natali et al. [24], martensite nucleation would take place after cold deformation up to 12.5 % on Cu23.89Zn4.8Al wt. %. Nevertheless, a deeper investigation using electric resistance measurement (ERM), transmission electron microscope (TEM), or other methods is needed in order to make further conclusion regarding the deformation-induced martensitic transformation.

3.3 Annealing behavior

Microstructures after annealing the specimens with the highest thickness reduction level (50 %) at various temperatures are shown in Fig. 4. Fig. 4 (b, d, f) shows that the α-matrix was also occupied by precipitates. According to Ahlers [16], these precipitates may form due to the presence of external stress or temperature. However, referring to the Cu-Zn binary phase diagram by Liang and Schmid-Fetzer [14], temperature drop below 400 °C would shift α/β phase boundaries further apart, encouraging precipitation of one phase in another. Furthermore, at higher temperature, e.g. 400 °C, the precipitates would coarsen as seen in Fig. 4 (f). However, the identities of these precipitates could not be confirmed in this study. At 600 °C (Fig. 4 (g-h)), deformation traces and precipitates which previously were found in the α-phase after deformation were much less visible, while recrystallized β′ grains were then observed in the optical micrograph. According to a work by Farabi et al. [31], the beta order-disorder reaction (β′ → β) would be fully completed at 570 °C and since β has lower activation energy (174 kJ/mol) than α (415 kJ/mol), recrystallization would only take place in β′ due to its lower activation energy. Some annealing twins were also visible in the β′ grains as seen in Fig. 4 (g), marked with red arrows. According to Zhang et al. [7], annealing twins were formed during recrystallization, driven by minimizing total excess energies of boundaries separating newly formed grains. Recrystallization was only observed in the light region as seen in Fig. 4 (g), therefore annealing twins were only visible in the recrystallized β′.

Evidence of recrystallization and annealing twins in β′ led to a conclusion that the possibility of β′ undergoing deformation during cold rolling existed. Xiao et al. [26] found nano-scale mechanical twinning in a cryogenic-plastically deformed Cu32Zn wt. %. The presence of nanotwining would significantly hinder dislocation movement in β′, giving significant internal stress that could furthermore become the driving force for recrystallization to happen [32].

3.4 Microhardness

Fig. 5 shows the overall microhardness of the Cu29.5Zn2.5Al wt. % alloy after cold rolling. An increase of hardness was found with increased deformation. This strengthening was attributed to a strain hardening effect in which dislocation movement was inhibited by dislocation pile-ups [30]. The suspected nanotwinning in β′ could also be responsible for the hardness increase by its ability to act as barriers for dislocation movement, as well as to increase alloys strain hardening rate [32]. Fig. 6 shows the hardness after annealing at different temperatures. Specimens annealed at 300 °C, 400 °C, and 600 °C experienced a conventional softening attributed to stress relief and the dislocation disentanglement mechanism [33]. This phenomenon is often observed after annealing cold-deformed Cu28Zn wt. % and Cu28Zn*x*Al wt. % alloys [8, 13]. On the other hand, specimens annealed at 150 °C exhibited hardening with microhardness of 234 ± 1 HV. Gong et al. [13] reported this strengthening effect for low-temperature annealing of cryorolled Cu20.8Zn2.14Al wt. % alloy at 150 °C and 200 °C for 30 min. They concluded that atom segregation to lattice defects (dislocations, stacking faults, twin boundaries, etc.) and along grain boundaries were responsible for the hardness increase.

It was presumed that the strengthening in the specimen annealed at 150 °C was caused either by a solute segregation (similar to the dislocation hindering mechanism by Cottrell atmosphere formation) as reported by Gong et al. [13] and Nestorović and Marković [34] in the investigation of annealed Al-brass at 200-400 °C after 60 % deformation or by the emergence of precipitates. To determine the presence of solute segregation, energy dispersive X-ray spectroscopy (EDX) was conducted with the results presented in Fig. 7 and Table 4. Composition analyses on grain boundary area show that the contents of Zn and Al were similar to β′ and were lower than α + precipitates area. This indicated that grain boundary segregation was not responsible for the unusual low-temperature anneal hardening effect. From the EDX analyses, it was also shown that

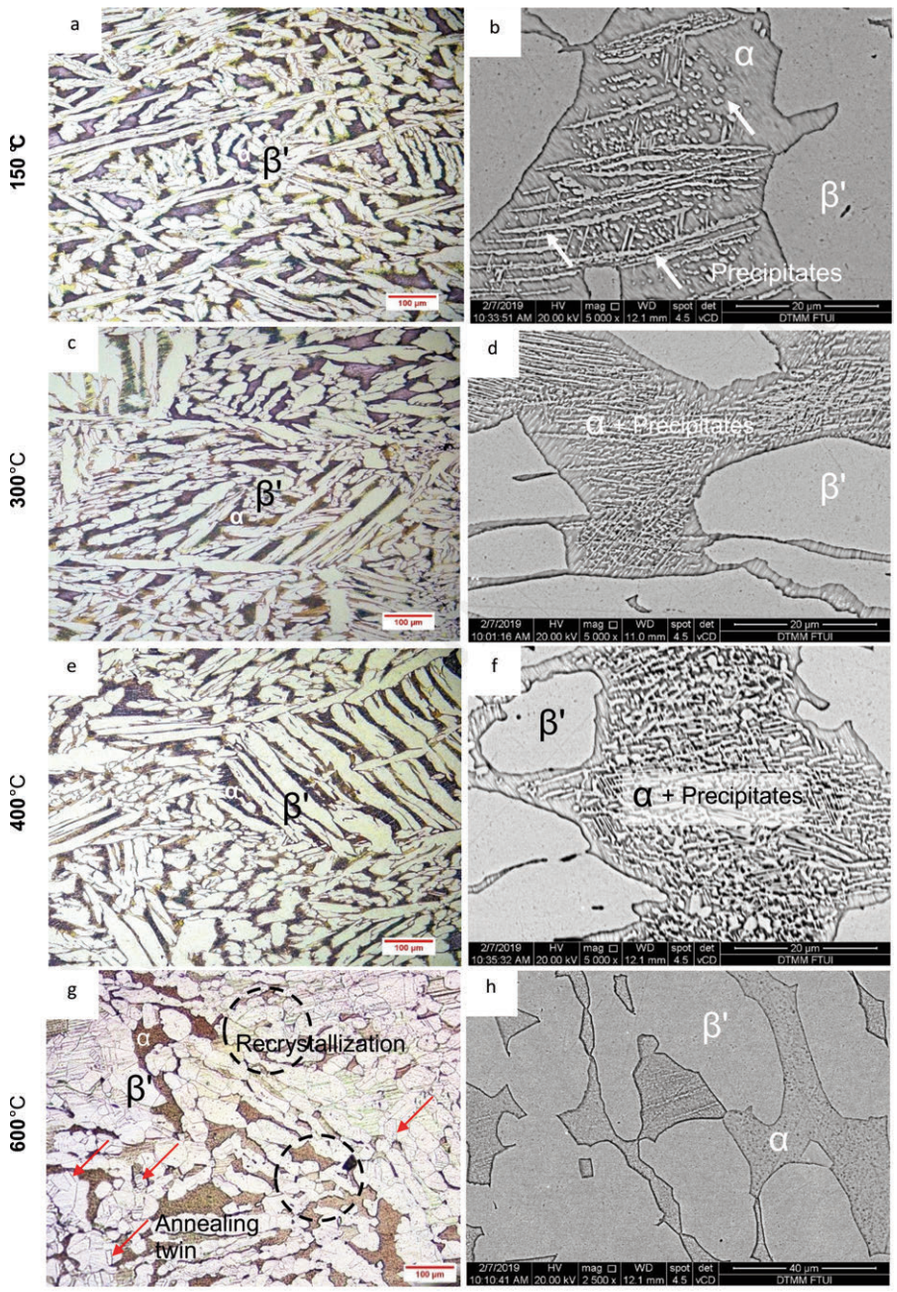

Figure 4. *Optical and Critical Dimension/CD-SEM images of the microstructures of 50 %-rolled Cu29.5Zn2.5Al wt. % annealed at (a-b) 150; (c-d) 300, (e-f) 400; and (g-h) 600 °C for 30 min, indicating precipitation in matrix, recrystallized β', and annealing twins*

the α region had higher Zn and Al contents than β′, which was assumed to happen due to the presence of precipitates in α. Hence, it was concluded that precipitates were the cause of the hardening in specimen annealed at 150 °C. At higher temperature (> 300 °C), stress relief became more significant than the hardness increase caused by precipitation, resulting in decreased hardness. Furthermore, it was assumed that the precipitates dissolved into the matrix at 600 °C since they were less visible (Fig. 4 (g)), thus a steep hardness decrease was observed.

Results of microhardness measurement of each α and β′ at different conditions are presented in Fig. 8. Both α and β′ experienced high strain hardening after 50 % cold rolling, confirming that the subjected deformation load was distributed in the two phases. The visible β′ phase had a more significant hardness increase after deformation, although deformation was only found in the α-phase region. The hardness increase in β′ was possibly due to nanotwinning in β′

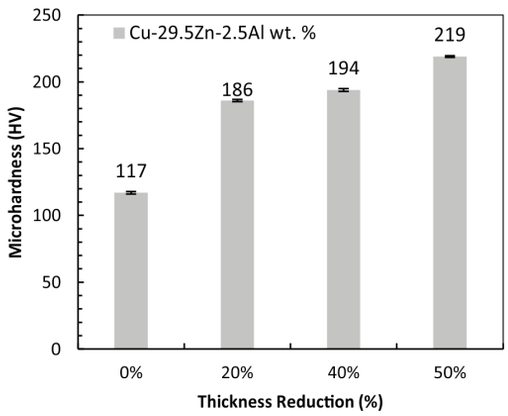

Figure 5. *Microhardness increase of as-homogenized Cu29.5Zn2.5Al wt. % observed simultaneously with higher cold deformation level*

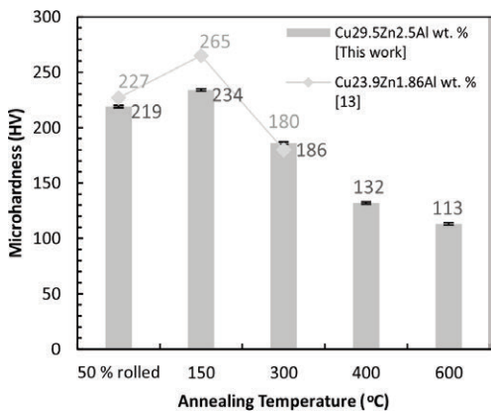

Figure 6. *Effect of annealing temperature on microhardness of 50 %-rolled Cu29.5Zn2.5Al wt. % showing unusual hardening at 150 °C and hardness decrease at 300 °C and above*

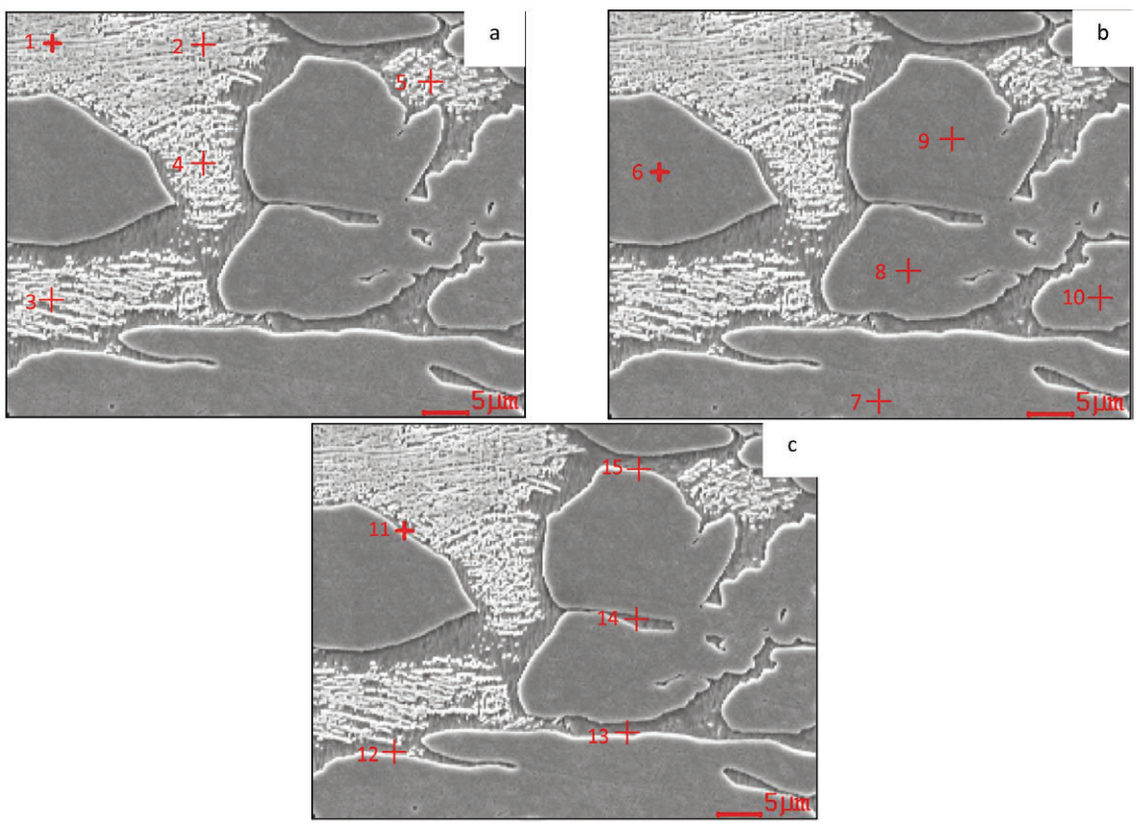

Figure 7. *Locations of EDX analyses on secondary electron-SEM images of the Cu29.5Zn2.5Al wt. % annealed at 150 °C: (a-b) spectra 1-5 in two-phase regions; (c-d) spectra 6-10 in dark regions; (e-f) spectra 11-15 at phase boundaries, with results shown in Table 4*

Table 4. *EDX results on Cu29.5Zn2.5Al wt. % alloys subjected to 50 % cold rolling and annealing at 150 °C for 30 min*

Spectrum	Composition (wt. %)			Phase
	Cu	Zn	Al	
5-Jan	65.1 ± 0.4	31.5 ± 0.4	3.4 ± 0.3	α + Precipitates
10-Jun	69.9 ± 0.7	27.1 ± 0.5	2.9 ± 0.2	β′
15-Nov	69.6 ± 0.5	27.5 ± 0.4	2.9 ± 0.2	Phase boundary

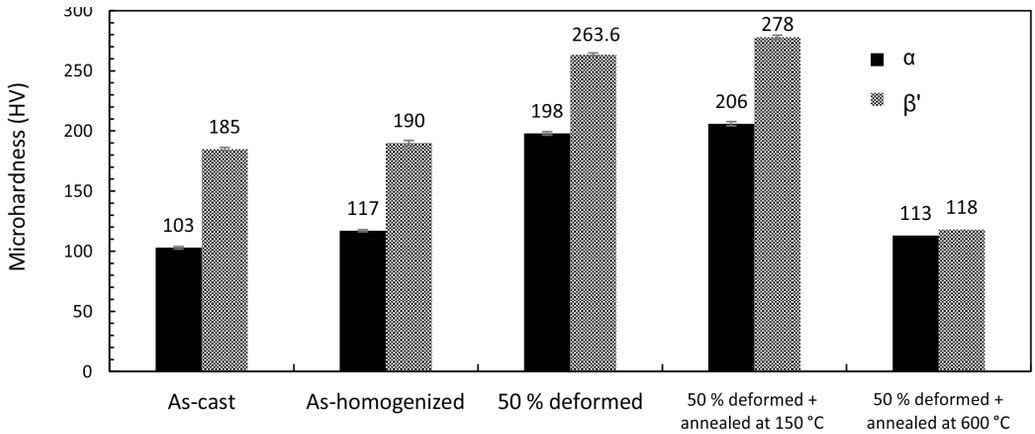

Figure 8. *Microhardness of α and β′ in Cu29.5Zn2.5Al wt. % alloys in various conditions*

during deformation as mentioned by Wang et al. [32], although future investigations using EBSD/TEM are needed to confirm this. Furthermore, annealing at 600 °C (~0.5 T_m) reduced the hardness in β′ due to the formation of stress-free phase through recrystallization. In particular, martensitic β′ was replaced with new equiaxed phases as observed in Fig. 4 (g-h), resulting in significantly lower microhardness. Hardness decrease in α is attributed to stress recovery mechanism.

4. Conclusions

An investigation was done on the effect of cold rolling and the variation of annealing temperature on the characteristics of α and β′ phases in gravity cast Cu29.5Zn2.5Al wt. % alloy, with the results as follows:

1. Cu29.5Zn2.5Al wt. % alloy consisted of α and β′ phases with α:β′ ratio of 35:65 in as-cast and as-homogenized samples.

2. Cold rolling increased overall microhardness of the alloys from 117 ± 0.95 to 186 ± 0.84, 194 ± 1.05, and 219 ± 0.63 HV after 20, 40, and 50 % thickness reduction, respectively. Traces of deformation mechanism, i.e. slip, intersecting slip bands, and shear bands were only visible in the α-phase region. However, β′ underwent an increase of microhardness from 190 ± 2.07 to 264 ± 1.36 HV after 50 % reduction.

3. Low-temperature annealing at 150 °C for 30 min. resulted in increased hardness of deformed samples from 219 ± 0.63 to 234 ± 0.89 HV, probably due to the formation of precipitates.

4. Microhardness of deformed alloys after annealing at 300, 400, and 600 °C were 186 ± 1.41, 132 ± 1.30, and 113 ± 0.95 HV, respectively, indicating a softening phenomenon attributed to stress relief and dislocation disentanglement.

5. β′ recrystallization was visible after annealing at 600 °C, causing a notable microhardness decrease from 264 ± 1.36 to 118 ± 1.70 HV due to the formation of equiaxed, stress-free grains.

6. XRD showed that deformation-induced martensites were present after 20 % cold rolling due to martensitic transformation in α-phase.

7. β′ martensites were present in α-phase after annealing at 150-400 °C due to a temperature-induced solid state transformation.

Acknowledgements

This research is financially supported by the Directorate of Research and Social Services of Universitas Indonesia through Hibah Publikasi Internasional Terindeks untuk Tugas Akhir (PITTA) 2018 with contract no. 2402/UN2.R3.1/HKP.05.00/2018.

References

[1] I. Basori, H. I. Pratiwi, B. T. Sofyan, Mater. Sci. Forum, 917 (2018) 212-217.

[2] I. Basori, I. Angela, D. Jendra, B. T. Sofyan, IOP Conf. Ser.: Mater. Sci. Eng., 378 (2018) 012015.

[3] A. Arisgraha, I. Angela, N. A. Arandana, B. T. Sofyan, IOP Conf. Ser.: Mater. Sci. Eng., 285 (2018) 012031.

[4] N. H. B. Minhat, Investigation of Brass Microstructure and Mechanical Properties using Metal Casting, Universiti Malaysia Pahang, Pahang, 2010, p. 4.

[5] S.V. Smirnov, M. V. Myasnnikova, N. B. Pugacheva, Int. J. of Damage Mech., 25 (2016) 251-265.

[6] Y. Mo, Y. Jiang, X. Liu, J. Xie, J. Mater. Process. Tech., 235 (2016) 75-84.

[7] X. K. Zhang, X. Y. Yang, W. Chen, J. Qin, J. P. Fouse, J. Alloys and Compounds, 679 (2016) 400-407.

[8] B. T. Sofyan I. Basori, ARPN J. Eng. App. Sci., 11 (2016) 2741-2745.

[9] T. Konkova, S. Mironov, A. Korznikov, G. Korznikova, M. M. Myshlyaev, S. L. Semiatin, Mater. Char., 101 (2015) 173-179.

[10] T. Wu, C. S. Hartley, X. M. Wang, C. T. Tsai, J. Mater. Process. Tech., 45 (1994) 111-116.

[11] J. Ulaganathan R. C. Newman, Mater. Char., 92 (2014) 127-137.
[12] R. Kumar, S. M. Dasharath. P. C. Kang, C. C. Koch, S. Mula, Mater. Des., 67 (2015) 637-643.
[13] Y. L. Gong, S. Y. Ren, S. D. Zeng, X. K. Zhu, Mater. Sci. Eng. A, 659 (2016) 165-171.
[14] S. M. Liang R. Schmid-Fetzer, CALPHAD: Comp. Coupling of Phase Diag. and Thermochem., 52 (2016) 21-37.
[15] K. K. Alaneme, E. A. Okotete, N. Maledi, J. Mater. Res. Tech., 6 (2017) 136-146.
[16] M. Ahlers, Progress in Mater. Sci., 30 (1986) 135-186.
[17] T. H. Grgurić, D. Manasijević, S. Kožuh, I. Ivanić, Lj. Balanović, I. Anžel, B. Kosec, M. Bizjak, M. Kneževic, M. Gojić, J. Min. Metall. Sect. B-Metall., 53 (3) B (2017) 413-422.
[18] C. M. Wayman T. W. Duerig, An Introduction to Martensite and Shape Memory, Raychem Corporation, California, 1990, pp. 3-20.
[19] P. R. Swann H. Warlimont, Acta Metall., 11 (1963) 511-517.
[20] O. A. Yakovsteva, A. V. Mikhaylovskaya, A. V. Pozdniakov, A. D. Kotov, V. K. Portnoy, Mater. Sci. Eng. A, 674 (2016) 135-143.
[21] N. Haberkorn, F. C. Lovey, A. M. Condó, J. Guimpel, Mater. Sci. Eng. B, 170 (2010) 5-8.
[22] R. Dasgupta, A. K. Jain, P. Kumar, S. Hussein, A. Pandey, J. Mater. Res. Tech., 3 (2014) 264-273.
[23] V. Asanović, K Delijić, N. Jauković, Scripta Mat., 58 (2008) 599-601.
[24] S. Natali, V. Volpe, L. Zortea, Convegno Nazionale Gruppo Italiano Frattura (IGF) XXII 1 (2013) 132-139.
[25] Y. H. Zhao, X. Z. Liao, Y. T. Zhu, Z. Horita, T. G. Langdon, Mater. Sci. Eng. A, 410-411 (2005) 188-193.
[26] G. H. Xiao, N. R. Tao, K. Lu, Mater. Sci. Eng. A, 513-514 (2009) 13-21.
[27] W. Q. Yuan, J. N. Wang, J. Mater. Process. Tech., 123 (2002) 31-35.
[28] R. S. Hay, Philosophical Mag., 88 (2008) 4243-4270.
[29] S. Suwas, R. K. Ray, Crystallographic Texture of Materials, Springer-Verlag, London, 2014, pp. 95-102.
[30] O. Engler and D. J. Jensen, Script. Met. Mater., 30 (1994) 25-30.
[31] E. Farabi, A. Zarei-Hanzaki, M. H. Pishbin, M. Moallemi, Mater. Sci. Eng. A., 641 (2015) 360-368.
[32] Y. Wang, M. Chen, F. Zhou, E. Ma, Nature 419 (2002) 912-917.
[33] R. Garg, S. Ranganathan, S. Suwas, Mater. Sci. Eng. A., 527 (2010) 4582-4592.
[34] S. Nestorović and D. Marković, Mater. Transactions, 40 (1999) 222-224.

UTICAJ HLADNOG VALJANJA I ŽARENJA NA KARAKTERISTIKE α + β′ FAZA KOD LEGURE Cu-29.5Zn-2.5Al DOBIJENE POSTUPKOM GRAVITACIONOG LIVENJA

I. Angela [a], I. Basori [b], B. T. Sofyan [a,*]

[a] Univerzitet u Indoneziji, Odsek za metalurgiju i materijale, Fakultet tehničkih nauka, Depok, Indonezija
[b] Državni univerzitet u Džakarti, Odsek za mašinsko inženjerstvo, Fakultet tehničkih nauka, Džakarta, Indonezija

Apstrakt

Legura aluminijuma i mesinga (Cu29.5Zn2.5Al wt. %) dobijena postupkom gravitacionog livenja podvrgnuta je postupku homogenizacije na 800°C u periodu od 2h prilikom koje je dobijena binarna kubična faza α i martenzitna β' faza koje su identifikovane primenom rentgentske difrakcije (XRD). Uzorci su nakon toga podvrgnuti postupku hladnog valjanja i žarenja na 150, 300, 400 i 600°C u periodu od 30 minuta. Na slikama mikrostrukture uzoraka nakon svake progresivne faze deformacije vidljivi su tragovi klizanja, trake klizanja koje se ukrštaju, kao i pojasevi smicanja. Martenzit nastao deformacijom se pojavio nakon 20% hladnog valjanja. Veća redukcija debljine dovela je do simultanog otvrdnjavanja faza. Žarenje na niskim temperaturama je proizvelo blago povećanje mikrotvrdoće i α i β' faze koje se dogodilo zbog formiranja taloga. SEM-EDX analiza je pokazala da u žarenim uzorcima nije došlo segregacije. Prilikom žarenja na višim temperaturama došlo je do uobičajenog omekšavanja. Ponovo kristalizovana ravnoosna zrna β' faze su bila vidljiva nakon žarenja na 600 °C.

***Ključne reči**: Aluminijum; Mesing; Homogenizacija; Martenzit; Hladno valjanje; Žarenje*